

Title: Bamboozled! Resolving deep evolutionary nodes within the phylogeny of bamboo corals (Octocorallia: Scleralcyonacea: Keratoisididae)

Authors: Declan Morrissey^{a*}, Jessica D Gordon^b, Emma Saso^c, Jaret P. Bilewitch^d, Michelle L. Taylor^b, Vonda Hayes^e, Catherine S. McFadden^f, Andrea M. Quattrini^c, & A. Louise Allcock^a

Affiliations

^a Ryan Institute & School of Natural Sciences, University of Galway, University Road, Galway, Ireland

^b School of Life Sciences, University of Essex, Colchester, United Kingdom

^c Department of Invertebrate Zoology, National Museum of Natural History, Smithsonian Institution, Washington, DC 20560, USA

^d National Institute of Water & Atmospheric Research Ltd (NIWA), 301 Evans Bay Parade, Wellington 6021, New Zealand

^e Department of Fisheries and Oceans, St. John's, Newfoundland and Labrador, Canada

^f Department of Biology, Harvey Mudd College, 1250 N. Dartmouth Ave., Claremont, CA 91711, USA

* d.morrissey4@universityofgalway.ie

Abstract

Keratoisididae is a globally distributed, and exclusively deep-sea, family of octocorals that contains species and genera that are polyphyletic. An alphanumeric system, based on a three-gene-region phylogeny, is widely used to describe the biodiversity within this family. That phylogeny identified 12 major groups although it did not have enough signal to explore the relationships among groups. Using increased phylogenomic resolution generated from Ultraconserved Elements and exons (i.e. conserved elements), we aim to resolve deeper nodes within the family and investigate the relationships among those predefined groups. In total, 109 libraries of conserved elements were generated from individuals representing both the genetic and morphological diversity of our keratoisidids. In addition, the conserved element data of 12 individuals from previous studies were included. Our taxon sampling included 11 of the 12 keratoisidid groups. We present two phylogenies, constructed from a 75% (231 loci) and 50% (1729 loci) taxon occupancy matrix respectively, using both Maximum Likelihood and Multiple Species Coalescence methods. These trees were congruent at deep nodes. As expected, S1 keratoisidids were recovered as a well-supported sister clade to the rest of the bamboo corals. S1 corals do not share the same mitochondrial gene arrangement found in other members of Keratoisididae. All other bamboo corals were recovered within two major clades. Clade I comprises individuals assigned to alphanumeric groups B1, C1, D1&D2, F1, H1, I4, and J3 while Clade II contains representatives from A1, I1, and M1. By combining genomics with already published morphological data, we provide evidence that group H1 is not monophyletic, and that the division between other groups – D1 and D2, and A1 and M1 – needs to be reconsidered. Overall, there is a lack of robust morphological markers within Keratoisididae, but subtle characters such as sclerite microstructure and ornamentation seem to be shared within groups and warrant further investigation as taxonomically diagnostic characters.

Keywords

Keratoisididae, Ultraconserved Elements, systematics, octocorals, morphology, phylogenomics

1 Introduction:

Octocorals are ecologically important benthic species capable of forming dense aggregations that can be considered Marine Animal Forests (Orejas et al., 2022; Rossi et al., 2022, 2017). Colonies can house unique communities of commensal invertebrates (Buhl-Mortensen and Mortensen, 2004; Maxwell et al., 2022; Parimbelli, 2020) and host larvae of commercially important fish (Baillon et al., 2012) and of other invertebrate species (Neves et al., 2020). Octocorals also provide attachment surfaces for egg cases. For example, the eggs of cirrate octopuses have been observed on species of bubblegum corals (Vecchione, 2019) and colonies of *Chrysogorgia* (Shea et al., 2018), while catshark eggs have been observed wrapped around colonies of *Callogorgia delta* (Etnoyer and Warrenchuk, 2007). In the deep sea, aggregations of octocorals are also classified as Vulnerable Marine Ecosystems (VMEs) and are warranted legal protection where states and Regional Fisheries Management Organisations are encouraged to implement conservation strategies to protect areas identified as VMEs.

Mitochondrial *MutS* (*mtMutS*) is the most commonly sequenced gene region for octocorals due to its relatively high variability in comparison with other regions (France and Hoover, 2002; van der Ham et al., 2009). This octocoral-specific protein is involved in active mismatch repair, and is one of the reasons for the slow accumulation of mutations within the mitogenome (Bilewitch and Degnan, 2011; Muthye et al., 2022), which has reduced the usefulness of more common single-gene barcodes for octocorals e.g., *COI* (France and Hoover, 2002). Used in isolation, *mtMutS* does not distinguish between many congeneric species (McFadden et al., 2010; Quattrini et al., 2019) and even when used in tandem with other genetic markers, still fails to distinguish between some species (Baco and Cairns, 2012; McFadden et al., 2011). It is often used in first-sweep biodiversity surveys (Benayahu et al., 2012; Haverkort-Yeh et al., 2013), and sequences are being increasingly used as reference libraries in environmental DNA surveys (Everett and Park, 2018). Owing to the large amount of available *mtMutS* sequence data, it has been used with other mitochondrial and nuclear markers to reconstruct octocoral phylogenies; however, there has not been enough signal to resolve deep nodes within those studies (Breedy et al., 2012; Cairns and Wirshing, 2015; McFadden et al., 2006).

Target enrichment sequencing of Ultraconserved Elements and exons, hereafter collectively referred to as conserved elements, has been used to explore and resolve the evolutionary histories of a wide range of taxa (Andersen et al., 2019; Faircloth et al., 2013; McCullough et al., 2019; Roxo et al., 2019). More recently, phylogenies constructed from conserved elements have revolutionised our understanding of octocoral systematics (see McFadden et al., 2022) and given unparalleled insight into the evolution of corals through their ability to resolve deep nodes (McFadden et al., 2021; Quattrini et al., 2020). Conserved element phylogenies have been shown to outperform those generated by traditional multi-locus methods (Blaimer et al., 2015).

While a low-resolution single gene barcode and lack of taxonomic expertise in many octocoral groups contribute to a lack of robust species-level identifications of octocorals in the literature, it is also recognised that many traditional morphological features that were once thought to be phylogenetically informative are evolutionarily labile. For example, for taxa that lack an axis, a stoloniferous or membranous colony growth form can be plastic within species or vary by population (McFadden et al., 2022). Among octocorals with an axis, branching patterns were once considered taxonomically informative, however, in some groups these characters are labile (Dueñas and Sanchez, 2009; France, 2007), and can result from convergent evolution (Quattrini et al., 2020; Sanchez et al., 2003). Species have also been identified that lack any recognized morphological, ecological, or geographic differentiation further questioning the usefulness of many taxonomic traits (McFadden et al., 2017).

Bamboo corals, which we use herein to refer to the family Keratoisididae, are one of four families (Chelidonisididae, Keratoisididae, Isididae, and Mopseidae) that have an articulated axis comprising an alternating sequence of proteinaceous nodes and calcium carbonate internodes. Until a revision in

2021 (Heestand Saucier et al., 2021), members of these families were classified in a single polyphyletic group (Kükenthal, 1919; Heestand Saucier et al., 2021) based on this distinct jointed axis. Members of Keratoisididae – globally distributed and exclusively deep sea (Watling et al., 2011) – are easily distinguishable from other articulated corals by their sclerome which comprises needles, spindles, rods, and scales. Previously, species were assigned to one of four genera solely on branching patterns: nodal branching in one plane was characteristic of *Isidella*; *Acanella* was diagnosed by nodal branching in multiple planes; species of *Keratois* branched from the internodes; and colonies that were unbranched were assigned to *Lepidisis*. Phylogenetic analyses of the keratoisidids have revealed that branching pattern is not diagnostic of any genus and that these genera are polyphyletic (Dueñas et al., 2014; France, 2007). New genera (Alderslade and McFadden, 2012; Lapointe and Watling, 2022; Watling, 2015; Watling and France, 2011) have been described to resolve some of the observed polyphyly, including *Adinisis* (Lapointe and Watling, 2022), *Cladarisis* (Watling, 2015), *Dokidisis* (Lapointe and Watling, 2022), *Eknomisis* (Watling and France, 2011), *Jasonisis* (Alderslade and McFadden, 2012), *Onkoisis* (Lapointe and Watling, 2022), *Orstomisis* (Bayer, 1990), and *Tanyostea* (Lapointe and Watling, 2022). The genus *Bathygorgia* has also been resurrected and placed within Keratoisididae (Lapointe and Watling, 2015). A three-locus phylogeny (*mtMutS*-5', *mtMutS*-3', and partial 18S) identified 12 distinct groups within the family, with varying levels of support (France, 2007; Watling et al., 2022) most of which have at least one genus that is typical of the group: A1 (*Acanella*), B1 (*Adinisis*), C1 (*Tanyostea*), D1, D2 (*Eknomisis* and *Keratois*), F1, G1 (*Bathygorgia*), H1 (*Onkoisis*), I1 (*Lepidisis* and *Isidella*), I4, J3 (*Dokidisis* and *Jasonisis*), M1 (*Orstomisis*), and S1 (*Cladarisis*). Many genera are still to be described. Each group has distinct morphological characters (e.g., polyp shape, sclerite composition, and distribution of polyps around the axis) that are considered typical (Watling et al., 2022). However, the phylogeny in Watling et al. (2022) did not have sufficient resolution to elucidate relationships among the defined groups and thus we are unable to identify key taxonomic features that characterise larger clades within the family.

Herein we (1) explore the use of target capture enrichment of conserved elements to resolve evolutionary relationships among Watling et al.'s (2022) alphanumerically defined groups within Keratoisididae, (2) compare phylogenomic trees constructed from conserved elements with those constructed using *mtMutS*, and previous phylogenies of the Keratoisididae, and (3) consider previously published morphologies of the keratoisidid groups in light of any novel relationships to elucidate any novel taxonomically informative characters.

2 Methods

2.1 DNA extraction, PCRs and *mtMutS* barcoding

Preserved tissue was received from the following museums and institutions, Canadian Museum of Nature (Canada), National Institute of Water and Atmospheric Research Invertebrate Collection (New Zealand), Museum of Comparative Zoology - Harvard University (USA), Museum of Tropical Queensland – Queensland Museum Network (Australia), Muséum national d'Histoire (France) National Museum of Natural History, Smithsonian Institute (USA) (Table S1). DNA was extracted from 166 bamboo corals using a modified salting out method (Miller et al., 1988) or a DNEasy Blood & Tissue kit (Qiagen) according to the manufacturer's instructions. For the salting out method, DNA was digested overnight at 65 °C with 7.5 µl of Proteinase K (20 mg/ml). Next, 2 µl of 100 mg/µl RNase A was added to the lysed DNA and incubated at 37 °C for 30 mins. 100 µl of 7.5 M ammonium acetate was added, followed by a 30-minute incubation on ice. The lysed DNA was then centrifuged at 16000 g for 15 minutes and the resulting supernatant transferred to a DNA low bind microcentrifuge tube. DNA was precipitated out of solution by the addition of 0.8x volume of chilled isopropanol and washed twice using 70% ethanol before being resuspended. DNA was quantified using a Qubit Fluorometer and checked for quality using a Nanodrop spectrophotometer.

A ~1000 bp region of *mtMutS-5'* was amplified for 77 individuals using previously published primers (Brugler and France, 2008; Sanchez et al., 2003) with the following thermocycling conditions: initial denaturation of DNA template at 94 °C for 5 mins followed by 35 cycles of 94 °C for 30 s, 55 °C for 30 s, and 72 °C for 45 s, with a final extension at 72 °C for 10 minutes (Brugler and France, 2008) or an initial denaturation step at 94 °C for 2 mins followed by 35 cycles 94 °C for 20 s, 50 °C for 30 s, and 72 °C for 50 s, with a final extension at 72 °C for 6 minutes (Brugler and France, 2008). For 74 specimens that had been previously sequenced, *mtMutS* sequences were downloaded from GenBank (Table S1). Sequences were aligned in MEGA X v 10.1.8 (Kumar et al., 2018) using MUSCLE (Edgar, 2004). The alignment was adjusted by eye so that codon-length gaps were in the correct position and did not change the amino-acid sequence.

Haplotype relationships were reconstructed using TCS v 1.21 (Clement et al., 2000) which implements a statistical parsimony method. Statistical parsimony is defined as the connectivity between the most closely related haplotypes based on a user-defined probability (Templeton et al., 1992). Gaps were coded as a 5th character state to include variability from indel structure.

2.2 Library preparation and target enrichment

One hundred and nine individuals representing the observed morphological and genetic diversity of available Keratoisididae specimens were selected for library preparation and target enrichment of conserved elements. For many specimens, eluted DNA was further purified using a DNEasy PowerClean Pro Cleanup Kit (QIAGEN) to remove PCR inhibitors and other impurities that may interfere with downstream processes.

Libraries were prepared and target enriched in-house or by Arbor BioSciences (Ann Arbor, MI, USA) as outlined in Quattrini et al. (2020, 2018) and the myBaits version IV protocol (Arbor BioSciences). 500 – 1000 ng of DNA for 15 samples was sent to Arbor BioSciences for library preparation and target enrichment. Ninety-four samples were prepared in-house for which approximately 700 ng of DNA from each individual was sheared to 400 – 800 bp using enzymatic fragmentation with a NEBNext® Ultra™ II FS DNA Module (#E7810, New England Biosciences) with a two-step digestion; 37 °C for 8 mins, and 65 °C for 30 mins. Libraries were then prepared using a Kapa Hyper Prep Kit (Roche), indexed using custom iTru dual-indexed primers (Glenn et al., 2019), and amplified with the following thermocycler conditions; 98 °C for 45 s, followed by 12 cycles of 98 °C for 15 s, 60 °C for 30 s, and 72 °C for 30 s, followed by a final extension at 72 °C for 1 min. For target enrichment, libraries were pooled into sets of eight and each set was enriched with the octocoral-specific RNA bait set (“octocoral-v2”) that targets 3,040 conserved elements (Erickson et al., 2021). Enriched libraries were sequenced on a HiSeq X Ten (150 bp, paired-end reads) by Quick Biology Inc (Pasadena, CA USA).

2.3 Bioinformatics and phylogenomic inferences

2.3.1 Conserved element recovery

Demultiplexed reads were processed using PhylUCE (Faircloth, 2016) by following tutorial one (<https://phyluce.readthedocs.io/en/latest/tutorials/tutorial-1.html>). Reads were trimmed using the illumiprocessor (Bolger et al., 2014; Faircloth, 2013) wrapper with default values and assembled using SPAdes (Bankevich et al., 2012) with the careful option (--careful) enabled, which performs a mismatch correction. Contigs from ten other keratoisidid bamboo corals and two specimens to be used as outgroups from previously published studies (McFadden et al., 2022; Quattrini et al., 2020, 2018) were included (Table S1). These additional specimens included sequences derived from the holotype of *Jasonis thresheri* (TMAG K3879). Baits targeting conserved elements were matched to the assembled contigs (70% identity, 70% coverage) using *phyluce_assembly_match_contigs_to_probes* to locate the targeted loci, which were then extracted using *phyluce_assembly_get_match_counts* and *phyluce_assembly_get_fastas_from_match_counts*, exported into separate FASTA files and aligned with default parameters using *phyluce_align_seqcap_align*, which implements MAFFT (Katoh and

Standley, 2013) and trims the edges of loci. Two data matrices of locus alignments were created using *phyluce_align_get_only_loci_with_min_taxa* in which each locus had 50% or 75% taxon occupancy.

2.3.2 Phylogenomic trees

Maximum Likelihood (ML) trees were constructed from the *mtMutS* haplotype data, and the concatenated alignment of conserved element loci within each taxon occupancy matrix using IQTree v 2.0.3. Nodal support for the haplotype tree was determined using 1000 non-parametric standard bootstraps (-b 100) with the best evolutionary model chosen by ModelFinder (Kalyaanamoorthy et al., 2017) as implemented inside IQTree (Nguyen et al., 2015). For each taxon occupancy matrix for the concatenated loci, the best model of evolution was determined using PartitionFinder's greedy heuristic algorithm, as implemented in IQTree, to determine whether partitions, which were initially by locus, should be merged during model selection (Appendix A2). Nodal support for the taxon occupancy matrix trees was determined by 1000 ultrafast bootstraps (-bb 1000).

Each locus alignment in both 50% and 75% taxon-occupancy datasets was input into IQTree for phylogenetic reconstruction. The best fit model of evolution for every locus was chosen by ModelFinder (Kalyaanamoorthy et al., 2017) and node support determined from 1000 ultrafast bootstraps (ufbs, -bb 1000). Nodes with support values less than 30 were collapsed from every tree using Newick Utilities (Junier and Zdobnov, 2010) and long branches were removed using Treeshrink (Mai and Mirarab, 2018). Species trees were then constructed from the individual trees in each of the 75% and 50% datasets using ASTRAL III v 5.7.8, a multispecies coalescent species tree method (Zhang et al., 2018). Node support was determined for the species tree from the Local Posterior Probability (LPP) which is the probability of a branch being a true branch based on the given set of gene trees. LPP values were transposed onto the nodes of the ML trees.

Where genera and species identity were unknown, we labelled our tree termini with the nomenclature established by France (2007) and expanded by Watling et al. (2022). This nomenclature describes the diversity of keratoisidids by their position within 12 major groups on a phylogenetic tree constructed from three gene regions (*mtMutS*-5', *mtMutS*-3', and 18S). To assign nomenclature to our tree termini, *mtMutS* sequences were compared with the curated database presented in Watling et al. (2022).

3 Results:

3.1 *mtMutS* phylogenetics

TCS recovered 44 unique haplotypes that represented 152 *mtMutS* sequences (14 individuals failed to amplify during PCR) across an 879 bp alignment. The *mtMutS* ML gene tree recovered the family Keratoisididae as monophyletic. Within Keratoisididae, one large well-supported clade, superclade α (Figure 1), comprised 17 haplotypes, many of which form soft polytomies when poorly supported (< 75 bs) nodes were collapsed. These polytomies included several single lineages and two well-supported clades consisting of multiple haplotypes corresponding to Watling et al.'s (2022) B1, C1, D1, D2, F1, and H1 groupings. Within superclade α , five haplotypes of D2 were recovered as monophyletic. Five B1 haplotypes were also monophyletic, but haplotype 34 fell outside the main B1 clade. The two D1 haplotypes were found to be sequential sisters to the Clade D2 and a B1 haplotype. The two H1 haplotypes were not recovered as a clade within superclade α . Two single lineages, C1 and F1, were also recovered as sequential sisters to the rest of superclade α on the phylogeny.

FIGURE 1 ABOUT HERE

Outside of superclade α , all seven J3 haplotypes formed a clade, as did the four and seven haplotypes referred to A1 and I1 respectively. Two specimens of M1 form a highly supported clade, which is itself a poorly supported sister to subclade A1. One specimen of M1, *Orstomisis crosnieri*, is a poorly

supported sister lineage to a larger A1 +M1 group. I4 was represented by a single specimen that also formed its own lineage.

3.2 Post-sequencing analyses and recovery of conserved element datasets

An average of $4\,039\,923 \pm 1\,622\,925$ (1SD) trimmed paired-end reads were recovered per sample post quality filtering. Trimmed reads were assembled into a mean of 31350 ± 25416 (1SD) contigs per sample with a mean length of 416 ± 88 bp. In total, 3007 conserved element loci were captured (out of the 3023 targeted) with an average of 1362 conserved elements per individual. The 75% and 50% taxon occupancy matrices contained 231 and 1729 loci respectively (Table 1).

TABLE 1 ABOUT HERE

3.3 Phylogenomic trees

ML trees using the 75% and 50% taxon occupancy matrices recovered Keratoisididae as monophyletic with S1 specimens sister to all other bamboo corals (Figure 2). Across both matrices, there were congruent relationships at deeper nodes which were supported by both high bootstrap and high LPP values. While the results of both conserved element trees support the overall larger pattern described by Watling et al. (2022), for example, the monophyly of many predefined keratoisidid groups, we primarily discuss incongruities between the trees below. The 50% matrix had more nodes with maximum bootstrap (100) and LPP (1) support on the maximum likelihood and species tree respectively compared with the 75% matrix (Figure 2).

FIGURE 2 ABOUT HERE

In both the 75% and 50% phylogenomic analyses, two reciprocally monophyletic clades (Clade I and Clade II) were recovered with maximum bootstrap and LPP support (Figure 2). Clade I comprised individuals assigned to B1, C1, D1, D2, F1, H1, I4, and J3. Clade II comprised specimens assigned to A1, I1 and M1 (Figure 2). We discuss incongruities between the two datasets in the description of these clades below.

3.3.1 Clade I

Within Clade I, two smaller clades were recovered. Clade I.i had maximum bootstrap and LPP support on both trees. Clade I.ii had maximum bootstrap support on both trees, maximum LPP support on the 50%-matrix tree, and high (>0.9) LPP support on the 75% tree. While Clade I.i, equivalent to superclade α in our *mtMutS* tree and Clade 5 from Watling et al (2022), contained two supported reciprocally monophyletic clades; one consisting of all C1 specimens and the other comprised D1 keratoisidids. Specimens assigned to Watling et al.'s (2022) B1, D2 and H1 were not recovered as monophyletic in this analysis. One of the H1 specimens was nested within a larger D1&D2 group, while the other nested within a clade consisting of B1 members. The relationship of D1 to the wider D2 groups was incongruent between the 75% and 50% trees. In the 75% matrix, D1 was supported as a sister clade to four D2 specimens (99 ufbs), and when poorly supported branches were collapsed (< 95 ufbs) that group formed a polytomy with a larger D2 clade. In the 50% matrix, D1 was found as a well-supported sister to all of those D2 corals. In both trees, an additional clade of D2 corals was recovered as sister to a clade of all other D1&D2 and one H1 specimen. All members of this additional clade of D2 corals were identified as *Eknomisis*. Since F1 was represented by a single sample, no conclusions can be drawn as to the monophyly of this group.

Clade I.ii comprised a maximally supported clade of J3 keratoisidids and a single lineage of I4. These were united by maximum bootstrap and LPP support on the 50% matrix, with > 0.9 LPP support for the 75% matrix. No equivalent to Clade I.ii was recovered in our *mtMutS* tree, instead J3 and I4 were in a soft polytomy with superclade α and A1, I1, and M1.

3.3.2 Clade II

Clade II comprised two reciprocally monophyletic clades, Clade II.i and Clade II.ii. Clade II.i contained all I1 representatives, which were also recovered as monophyletic in the *mtMutS* tree.

Clade II.ii comprised a fully supported clade of *Acanella* (A1), and representatives from Watling et al.'s (2022) M1. In the tree based on the 75% occupancy matrix, two individuals of M1 (NIWA86194 and MNHN-IK-2012-17005) formed a well-supported clade sister to subclade A1, with one M1 individual (NTM C014584, *Orstomisis crosnieri*) recovered as a well-supported sister taxon to those two clades. This relationship was observed in the *mtMutS* phylogeny, with haplotype 12 and haplotype 13 (NIWA86194 and MNHN-IK-2012-17005 respectively) recovered as sister taxa with maximum bootstrap support, and Haplotype 11 (*Orstomisis crosnieri*) on a separate branch from a poorly supported node. In the 50% matrix, NTM C014584 is sister to the A1 subclade, with the clade formed by NIWA86194 and MNHN-IK-2012-17005 sister to those two clades (A1 + NTM C014584).

4 Discussion:

This study is the first to use conserved elements to resolve deep evolutionary relationships among the previously defined subclades within Keratoisididae. Our study comprises 152 individuals sequenced at *mtMutS*, 121 of which have conserved element data. These 121 individuals span 11 of 12 previously defined groups, with only G1 absent from our analyses. Previous phylogenies (*mtMutS*-5', *mtMutS*-3', and 18S in Watling et al., 2022; *mtMutS*-5', 16S, and *igr4* in Dueñas et al., 2014; and *mtMutS*-5', *COI*+*igr1*, 16S-*nad2*, and *igr4* in Morrissey et al., 2022), including the single gene *mtMutS* presented herein, did not resolve deep nodes within the family. In contrast, there was congruence at all deep nodes in the 75% and 50% conserved element phylogenomic trees – which were all highly supported – with only the relationship among M1 specimens and the relationship of group D1 to D2 incongruent between trees. Our conserved element ML and ASTRAL phylogenies both returned the family Keratoisididae as monophyletic with representatives of S1 forming a well-supported sister clade to the rest of the family as expected due to their different mitochondrial gene order.

4.1 Taxonomic considerations

Morphological characteristics of each major group have been previously published (table 4, Watling et al. 2022). However, due to the low resolution of the relationships among groups in Watling et al. (2022), it was impossible to map morphological traits to the deeper nodes. Our conserved elements tree has resolved the relationship among 11 of 12 major groups, yet many reported morphological traits are still not synapomorphies of any single group or evolutionary lineage (Figure 3). For example, Clade I.i is made up of internodal branchers (except F1 which can be nodal or internodal) and Clade I.ii contains both nodal and internodal branchers (Figure 3). Members of J3 (found in Clade I.ii) can have both nodal and internodal branching on the same colony or completely lack any proteinaceous nodes (Watling et al., 2022). Clade II comprises nodal branchers (Figure 3). Other morphological characters that are widely variable throughout the conserved elements tree include colony shape. Many different subclades have species with diverse colony forms that vary from whips to bushes (e.g., D1, D2, and J3), include fans (e.g., B1 and I1) and are not exclusive to either Clade I or Clade II (Figure 3). Other characters such as coenenchyme thickness are also highly variable with both thick and thin coenenchyme found in Clade I and just thin coenenchyme in Clade II (Figure 3). A recent revision of Octocorallia suggests that reclassification of taxa at, and above, the rank of family should not focus on gross morphological traits (e.g., colony forms, skeletal morphology, and branching patterns, as outlined above) but instead on more subtle characters that are shared in well-supported molecular clades (McFadden et al., 2022). Our phylogeny suggests this may be true for the classification of taxa below the rank of family within Keratoisididae. Sclerite microstructures and

ornamentation (see below examples) seem to be widely shared within subclades while colony forms and branching patterns are not diagnostic.

FIGURE 3 ABOUT HERE

4.2 Clade I

4.2.1 Clade I.i

4.2.2 Untangling D1 & D2

There are two currently accepted genera within D2: *Eknomisis* and *Keratoisis*. *Eknomisis* was described in 2011 and, like *Keratoisis* which was described in 1869, it branches from the internodes (Watling and France, 2011). Previous molecular phylogenies, and our *mtMutS* phylogeny, have recovered *Eknomisis* nested within the larger *Keratoisis* D2 group (Dueñas et al., 2014; Morrissey et al., 2022; Watling et al., 2022). In both our 50% and 75% conserved elements phylogenomic inferences, all individuals tentatively identified as *Eknomisis* from Morrissey et al. (2022) and USNM1516861 (identified as *Eknomisis* due to similarity in polyp morphology and sclerite arrangement to *Eknomisis* sp., figure S6 in Morrissey et al. (2022)) form a distinct clade that is sister to the wider D1&D2 (including H1 representative NIWA106530) group. *Eknomisis* is distinct from *Keratoisis* due to its oblique arrangement of sclerites along the polyp body and some individuals having distinct volcano-shaped polyps (which may be absent if the polyps were not fully contracted or fully formed) when preserved (Watling and France, 2011). Other members of D2 have sclerites that are usually arranged longitudinally and obliquely, or unaligned along the polyp. Individuals within the *Eknomisis* clade have varying colony morphologies (see figures S4-S6 in Morrissey et al. 2022). This suggests that sclerite arrangement is a robust character for diagnosing *Eknomisis* even among a range of colony morphologies.

The relationships among D1 and D2 groups are incongruent between our 50% and 75% phylogenies. If nodes with <70% support had been collapsed on the Watling et al. (2022) phylogeny, then D1 and D2 would have appeared intermixed, forming a polytomy comprising a D2 clade, a D1 clade and a separate lineage of D1. This, in addition to the incongruence in our conserved elements trees, suggests that the division of D1 and D2 may not be warranted. The typical morphologies of D1 and D2 members described in table 4 of Watling et al. (2022) differ only in (i) the polyp arrangement around the axis: D2 has polyps originating from all around the axis while D1 has polyps on one or two sides most commonly, and (ii) sclerite composition in the polyp body: D1 has needles which are usually sparse in the bottom half of the polyp, while D2 has needles and rods and that are found in both the upper and lower parts of the polyps. The latter difference is not always present, for example USNM1593473 is placed within D1 based on molecular data yet it has polyps that are heavily armoured with needles (see figure S8 Morrissey et al. 2022).

Finally, USNM1593494 was identified as a member of D2 as its *mtMutS* sequence is identical to the sequence derived from a D2 specimen *Keratoisis ?fruticosa* (GenBank accession No. KX362335.1), but its position in our phylogeny is incongruent between our 75% and 50% conserved elements analyses. In the phylogeny based on the 75% occupancy matrix, USNM1593494 is sister taxon to a larger D1 and D2 group, and in the phylogeny based on the 50% occupancy matrix, it is found within the D2 clade. Despite, the *mtMutS* sequence suggesting this specimen belongs in D2, the polyp sclerite morphology of USNM1593494 (see figure S7 in Morrissey et al. 2022) is consistent with that described for Watling et al.'s (2022) D1: needles that are sparse in the bottom half of the polyp, suggesting that there is no robust division between subclades D1 and D2.

4.2.3 Untangling H1

Within our *mtMutS* and 50% and 75% conserved elements trees, the two specimens representing Watling et al.'s (2022) H1 (NIWA26595 and NIWA106530) did not form a clade. As currently defined, H1 comprises two species, *Onkosis solitaria* and *Onkosis magnifica*. The *mtMutS* sequence

derived from NIWA26595 was 99.86% similar to the sequence from the holotype of *Onkoisis solitaria* (= *Lepidisis solitaria*) (GenBank accession No. KC660851). In both conserved elements phylogenies presented here, NIWA26595 was nested within B1. The *mtMutS* sequence of NIWA106530 is identical to that of the holotype of *O. magnifica* (= *Keratoisis magnifica*) (GenBank accession No. KC660852) and was recovered in both conserved elements phylogenies within the larger D1&D2 group (Figure 2). Previous phylogenies that included both *O. magnifica* and *O. solitaria* have been incongruent. Watling et al. (2022), using *mtMutS*-5', *mtMutS*-3', and partial 18S rRNA, recovered these two species as sister taxa, and erected the moderately supported (BS 71, BI 0.6) H1. Dueñas et al. (2014) found these two species to be distantly related using *mtMutS*-5', 16S, and *igr4*.

Onkoisis magnifica shares some morphological characters with the wider D1&D2 group. For example, *O. magnifica* and all members of D1&D2 branch from the internodes and have blunt-ended rods along the tentacles (Figure 3). These rods have heavy ornamentation in the form of ridges at both ends of the sclerite e.g. *Keratoisis fruticosa* (D1, see figure 7 Lapointe and Watling, 2022), *Keratoisis ramosa* (D1, see figure 10 in Lapointe and Watling, 2022), and other undescribed species within the D1&D2 subclade (see figures S1-S9 Morrissey et al., 2022). *Onkoisis magnifica* also has this ornamentation at the ends of the tentacle sclerites (see figure 5 Dueñas et al., 2014). Both *O. magnifica* and members of D1&D2 have polyp and coenenchyme sclerites that are longitudinally striated (see aforementioned figures).

The reclassification of *Lepidisis solitaria* to the genus *Onkoisis* was due to its observed sister relationship with *O. magnifica* on Watling et al.'s (2022) phylogenetic tree and not due to shared morphological characters, as the morphology of the holotype was not examined in detail during reclassification (Lapointe and Watling, 2022). *Onkoisis solitaria* contains scale-shaped sclerites in the body of the polyp and coenenchyme (Grant, 1976), a character seen in the genus *Adinisis* (a member of B1, Lapointe and Watling, 2022), and in undescribed species referred to B1 in Morrissey et al. (2022) (see figures S10-S14 Morrissey et al., 2022). There is insufficient tissue of NIWA26595 and NIWA106530 for further detailed morphological examination so additional sequencing of the type material of both *O. magnifica* and *O. solitaria* is needed to further investigate their relationship to one another. However, it is possible that H1 is not a valid grouping and that the generic classifications of *O. magnifica* and *O. solitaria* need to be revised.

4.2.4 Clade I.ii

Previously published studies indicated that members of Clade I.ii show a wide range of polyp and sclerite morphologies (Watling et al., 2022). The sclerites of *Jasonisis* comprise scales with fluted margins in the polyp body (Alderslade and McFadden, 2012) while those of *Dokidisis* are blunt rods that appear striated (Lapointe and Watling, 2022). Our tree also includes J3 specimens with heavily granulated spindle-shaped sclerites in the polyp body (Morrissey et al. 2022; figures S23-25), suggesting the presence of at least three genera within our J3 specimens. Due to the range of morphologies present, it is currently difficult to identify synapomorphies for the wider J3 subclade without further thorough taxonomic investigations of more keratoisidids. Recently, it was suggested that all J3 specimens blacken when frozen or preserved in ethanol (Morrissey et al., 2022), as seen in *Jasonisis thresheri* and undescribed specimens from Ireland (Morrissey et al., 2022). However, we observed a J3 specimen (NIWA64445, *Jasonisis* sp.) that did not have blackened tissue, which suggests that while useful, it is not a synapomorphy and instead may be a physiological reaction due to stress when collected e.g., the tissue of *Paramuricea* species blackened when exposed to oil and oil dispersants (DeLeo et al., 2016) and it is also known to blacken when collected (Kenchington et al., 2009).

4.3 Clade II

4.3.1 Clade II.i

Both conserved element trees and the *mtMutS* phylogeny returned I1 as a clade. Watling et al. (2022) recovered *Lepidisis caryophyllia*, the type species for the genus *Lepidisis*, in this clade. *Lepidisis* is undergoing major revisions (Watling and France, 2021) as species currently assigned to this genus appear across multiple clades as lack of branching was traditionally used as the sole diagnostic trait of the genus. *Lepidisis* is now considered to contain species that are unbranched or branch from the nodes (Watling and France, 2021). While currently polyphyletic, the genus *Isidella* is also considered to be in Clade I1 (Watling et al., 2022). *Isidella* also branches from the nodes so until a thorough revision of both genera is complete, and type material sequenced, it is difficult to separate the genera. Our I1 clade contains both unbranched and nodal branching corals.

4.3.2 Clade II.ii

4.3.3 Untangling A1 and M1

In both the 75% and 50% conserved elements phylogeny, M1 is polyphyletic: in the 75% tree two individuals formed a clade that was a well-supported sister taxon to A1, while a third (NTM C014584) forms a well-supported sister taxon to the A1 (= *Acanella*) + other M1 clade. In the 50% conserved elements phylogeny, it is NTM C014584 that is found as a sister-taxon to A1, while the other two form a separate clade. In Watling et al.'s (2022) three-gene phylogeny, M1 was also polyphyletic: an M1 clade, a separate M1 lineage, and an I1 clade formed a trichotomy. In that study, A1 was found in the same Clade as M1 and I1 and J3 (referred to in that study as Clade 4), although the relationships among these groups was not resolved. Individuals identified as *Orstomisis crosnieri* (which are representative of M1) were recovered as sister taxa to a small clade comprising *Acanella* (=A1) in Dueñas et al. (2014). However, in that study, the genus *Acanella* was recovered as polyphyletic making inferences about the true relationship between *Orstomisis* (M1) and *Acanella* difficult.

The colony morphology of *Acanella* (A1) and *Orstomisis* (M1) differ greatly: *Acanella* forms colonies that vary in shape from flabellate to bushy and *Orstomisis* colonies are multi-planar flabellate. However, *Orstomisis* and *Acanella* do share more subtle morphological features: they both contain rods in the polyp body, with needles also being found in *Acanella*; and in both genera, there are varying degrees of granulation along the length of the body and tentacle sclerites (Bayer, 1990; see figures S26-29 Morrissey et al., 2022; Heestand Saucier et al., 2017), although granulation is not exclusive to these genera but is also seen in other groups across the family, for example, in undescribed species assigned to J3 (see figures S23-25 Morrissey et al., 2022). *Orstomisis* and *Acanella* also share a distinct mitochondrial genomic feature: the intergenic spacer *igr4*, between *cob* and *nad6*, is only 42 bp (van der Ham et al., 2009) whereas it is much longer in all other genera of keratoisidids sequenced.

4.4 Utility of studies with fewer loci

Next generation sequencing has allowed us to produce large genomic datasets that include variability from across the whole genome. These datasets have revealed hypotheses of species evolution that conflict with those derived from single- or multigene mitochondrial and nuclear data (Herrera and Shank, 2016; Pante et al., 2015; Quattrini et al., 2022a; Quattrini et al., 2019). While poor resolution from low variability within the single markers can cause phylogenetic uncertainty, mito-nuclear discordance is also prevalent within Anthozoa at all taxonomic levels, believed to be a result of recent and ancient introgression/hybridisation, and selection (Quattrini et al., 2022b). Incomplete lineage sorting has also been suggested as a major problem when inferring the true relationships of rapidly radiating groups, which may be the case with Keratoisididae. However, the presence of superclade alpha in our *mtMutS* phylogeny, which corresponds to Clade 5 from Watling et al. 2022 and Clade I.i in our conserved element phylogenies, suggests there is still some utility to using single gene markers for initial phylogenetic explorations.

Phylogenies based on the full mitogenomes of Keratoisididae are needed to determine whether there is mito-nuclear discordance or whether phylogenies that have used few mitochondrial markers just lack the resolution to resolve deeper relationships. This is important for informing how future studies (encompassing additional taxon sampling to solve taxonomic issues throughout Keratoisididae) are conducted.

Finally, while it is advised not to rely on single gene markers for both barcoding and inferring phylogenetic relationships within Octocorallia, the increasing interest in the use of eDNA as a non-invasive survey method (Alexander et al., 2020; Dugal et al., 2022; Everett and Park, 2018; Laroche et al., 2020) means that single-gene markers will continue to be used in the future. Therefore, it is still useful to compare these single-gene inferences with more robust inferences from conserved elements to determine any inconsistencies or similarities between the two methods. Single- or multigene barcoding are also still useful tools for species-level biodiversity surveys and can be used to identify colonies that warrant further investigation with both taxonomic and genomic tools.

5 Conclusion

Conserved elements have provided the genomic resolution necessary to determine the relationships among 11 of 12 previously defined groups within Keratoisididae, which all previous phylogenies, based on single or multiple genes, including our own *mtMutS* phylogeny, have been unable to do. By combining genomics with already published morphological data, we provide evidence that some groups (H1) are not monophyletic, and that the division between other groups – D1 and D2, and A1 and M1 – needs to be reconsidered. Overall, there is a lack of robust morphological markers within Keratoisididae, but subtle characters such as sclerite microstructures and ornamentation seem to be shared within groups and warrant further investigation as taxonomically diagnostic characters. The high support for deep nodes on these conserved elements based phylogenies will allow new morphological characters to be explored. This study included type material for only one species, *Jasonis thresheri*. Inclusion of further type material in future conserved elements based studies would provide significant support to revisions of genera and the resolution of species-level relationships.

Data Availability

Raw read data are available in NCBI Genbank SRA archive BioProject PRJNA994824 (Biosamples #SAMN36449194 - SAMN36449302). Newly generated *mtMutS* sequences were uploaded to NCBI GenBank (OR253813 - OR253887).

Acknowledgements

D Morrissey is funded by an Irish Research Council Postgraduate Scholarship GOIPG/2019/3682. This research was supported by a University of Galway Thomas Crawford Hayes Fund award and a Genetics Society UK training grant. The authors wish to acknowledge the Irish Centre for High-End Computing (ICHEC) for the provision of computational facilities and support under projects nglif036c, ngear020c, and nglif049b.

Access to specimens from Muséum National d'Histoire Naturelle was facilitated by Eric Pante and Magalie Castelin. Specimens were collected from cruises ATIMO VATAE, BIOMAGLO, PAPUA NIUGINI, SALOMON 2, and TERRASES. The authors wish to thank the Museum of Comparative Zoology Invertebrate Zoology Department and Cryogenic Collection for use of specimens/samples, the Queensland Museum, and the Canadian Natural Museum for access to specimens from their collections. Specimens provided by the Smithsonian Institution National Museum of Natural History that were used in this study came from CE13008 (ALA, chief scientist) CE14009 (M. White, chief scientist), and CE16006 (ALA, chief scientist) aboard the *RV Celtic Explorer* funded by the Irish National Ship Time Programme. Samples also came from research cruises CE17008 (ALA, chief

scientist) and CE18012 (ALA, chief scientist) aboard the *RV Celtic Explorer* which were funded by Science Foundation Ireland and the Marine Institute under Investigators Programme Grant SFI/15/IA/3100 and co-funded under the European Regional Development Fund 2014–2020 awarded to ALA. A few specimens were collected during the *R/V Atlantis* DEEPSEARCH cruise (E. Cordes, chief scientist), which was funded by the US Department of the Interior, Bureau of Ocean Energy Management. Access to specimens and data from the NIWA Invertebrate Collection were provided by Di Tracey and Sadie Mills (NIWA) and were collected on the following voyages: TAN0205 and KAH0204 - “Seamounts: their importance to fisheries and marine ecosystems”, undertaken by NIWA and funded by the former New Zealand Foundation for Research, Science and Technology (FRST) with additional funding from the former Ministry of Fisheries; TAN1003 - Orange Roughy trawl survey collected by NIWA and funded by Fisheries New Zealand (FNZ); TAN1007 - collected by NIWA during the Kermadec Arc Minerals (KARMA) voyage, funded by FRST, in collaboration with Auckland University, Institute of Geological and Nuclear Science (GNS Science), and Woods Hole Oceanographic Institute (WHOI); TAN1104 - Ocean Survey 20/20 Mapping the Mineral Resources of the Kermadec Arc Project, funded by Land Information New Zealand, GNS Science, NIWA, and WHOI; TAN1213 - Nascent Inter-Ridge Volcanic And Neotectonic Activity (NIRVANA) voyage, funded by the Ministry for Primary Industries, in collaboration with Auckland University, GNS Science, and the University of New Hampshire; Stations beginning with TRIP were collected under the Scientific Observer Program funded by FNZ, or in Antarctic waters by the Commission for the Conservation of Antarctic Marine Living Resources (CCAMLR).

The manuscript was greatly improved by the constructive and insightful comments of Les Watling and an anonymous reviewer.

Author contributions

Declan Morrissey: Conceptualization, Methodology, Formal analysis, Investigation, Data Curation, Writing - Original Draft, Writing - Review & Editing, Visualization, Funding acquisition. **Jessica D Gordon:** Methodology, Investigation, Writing - Review & Editing. **Emma Saso:** Methodology, Investigation, Writing - Review & Editing. **Jaret P. Bilewitch:** Resources, Writing - Review & Editing. **Michelle L. Taylor:** Resources, Writing - Review & Editing. **Vonda Hayes:** Resources, Writing - Review & Editing. **Catherine S. McFadden:** Resources, Writing - Review & Editing, Funding acquisition. **Andrea M. Quattrini:** Conceptualization, Data Curation, Writing - Review & Editing, Visualization, Supervision, Funding acquisition. **A. Louise Allcock:** Conceptualization, Formal analysis, Data Curation, Writing - Original Draft, Writing - Review & Editing, Visualization, Supervision, Funding acquisition.

References

- Alderslade, P., McFadden, C.S., 2012. A new genus and species of the family Isididae (Coelenterata: Octocorallia) from a CMAR Biodiversity study, and a discussion on the subfamilial placement of some nominal isidid genera. *Zootaxa* 3154, 21–39.
<https://doi.org/10.11646/zootaxa.3154.1.2>
- Alexander, J.B., Bunce, M., White, N., Wilkinson, S.P., Adam, A.A.S., Berry, T., Stat, M., Thomas, L., Newman, S.J., Dugal, L., Richards, Z.T., 2020. Development of a multi-assay approach for monitoring coral diversity using eDNA metabarcoding. *Coral Reefs* 39, 159–171.
<https://doi.org/10.1007/s00338-019-01875-9>
- Andersen, M.J., McCullough, J.M., Friedman, N.R., Peterson, A.T., Moyle, R.G., Joseph, L., Nyári, Á.S., 2019. Ultraconserved elements resolve genus-level relationships in a major Australasian bird radiation (Aves: Meliphagidae). *Emu - Austral Ornithol.* 119, 218–232.
<https://doi.org/10.1080/01584197.2019.1595662>

- Baco, A.R., Cairns, S.D., 2012. Comparing molecular variation to morphological species designations in the deep-sea coral *Narella* reveals new insights into seamount coral ranges. *PLoS One* 7, e45555.
- Baillon, S., Hamel, J.-F., Wareham, V.E., Mercier, A., 2012. Deep cold-water corals as nurseries for fish larvae. *Front. Ecol. Environ.* 10, 351–356.
- Bankevich, A., Nurk, S., Antipov, D., Gurevich, A.A., Dvorkin, M., Kulikov, A.S., Lesin, V.M., Nikolenko, S.I., Pham, S., Prjibelski, A.D., Pyshkin, A.V., Sirotkin, A.V., Vyahhi, N., Tesler, G., Alekseyev, M.A., Pevzner, P.A., 2012. SPAdes: a new genome assembly algorithm and its applications to single-cell sequencing. *J. Comput. Biol. J. Comput. Mol. Cell Biol.* 19, 455–477. <https://doi.org/10.1089/cmb.2012.0021>
- Bayer, F.M., 1990. A new isidid octocoral (Anthozoa: Gorgonacea) from New Caledonia, with descriptions of other new species from elsewhere in the Pacific Ocean.
- Benayahu, Y., Ofwegen, L., Dai, C.-F., Jeng, M.-S., Soong, K., Shlagman, A., Hsieh, H., McFadden, C., 2012. Diversity, Distribution, and Molecular Systematics of Octocorals (Coelenterata: Anthozoa) of the Penghu Archipelago, Taiwan. *Zool. Stud.* 51, 1529–1548.
- Bilewitch, J.P., Degnan, S.M., 2011. A unique horizontal gene transfer event has provided the octocoral mitochondrial genome with an active mismatch repair gene that has potential for an unusual self-contained function. *BMC Evol. Biol.* 11, 228. <https://doi.org/10.1186/1471-2148-11-228>
- Blaimer, B.B., Brady, S.G., Schultz, T.R., Lloyd, M.W., Fisher, B.L., Ward, P.S., 2015. Phylogenomic methods outperform traditional multi-locus approaches in resolving deep evolutionary history: a case study of formicine ants. *BMC Evol. Biol.* 15, 271. <https://doi.org/10.1186/s12862-015-0552-5>
- Bolger, A.M., Lohse, M., Usadel, B., 2014. Trimmomatic: a flexible trimmer for Illumina sequence data. *Bioinforma. Oxf. Engl.* 30, 2114–2120. <https://doi.org/10.1093/bioinformatics/btu170>
- Breedy, O., van Ofwegen, L.P., Vargas, S., 2012. A new family of soft corals (Anthozoa, Octocorallia, Alcyonacea) from the aphotic tropical eastern Pacific waters revealed by integrative taxonomy. *Syst. Biodivers.* 10, 351–359. <https://doi.org/10.1080/14772000.2012.707694>
- Brugler, M.R., France, S.C., 2008. The mitochondrial genome of a deep-sea bamboo coral (Cnidaria, Anthozoa, Octocorallia, Isididae): genome structure and putative origins of replication are not conserved among octocorals. *J. Mol. Evol.* 67, 125.
- Buhl-Mortensen, L., Mortensen, P.B., 2004. Crustaceans associated with the deep-water gorgonian corals *Paragorgia arborea* (L., 1758) and *Primnoa resedaeformis* (Gunn., 1763). *J. Nat. Hist.* 38, 1233–1247. <https://doi.org/10.1080/0022293031000155205>
- Cairns, S., Wirshing, H., 2015. Phylogenetic reconstruction of scleraxonian octocorals supports the resurrection of the family Spongiodermidae (Cnidaria, Alcyonacea). *Invertebr. Syst.* 29, 345–368. <https://doi.org/10.1071/IS14063>
- Clement, M., Posada, D., Crandall, K.A., 2000. TCS: a computer program to estimate gene genealogies. *Mol. Ecol.* 9, 1657–1659.
- DeLeo, D.M., Ruiz-Ramos, D.V., Baums, I.B., Cordes, E.E., 2016. Response of deep-water corals to oil and chemical dispersant exposure. *Deep Sea Res. Part II Top. Stud. Oceanogr.* 129, 137–147.
- Dueñas, L., Sanchez, J.A., 2009. Character lability in deep-sea bamboo corals (Octocorallia, Isididae, Keratoisidinae). *Mar. Ecol. Prog. Ser.* 397, 11–23. <https://doi.org/10.3354/meps08307>
- Dueñas, L.F., Alderslade, P., Sánchez, J.A., 2014. Molecular systematics of the deep-sea bamboo corals (Octocorallia: Isididae: Keratoisidinae) from New Zealand with descriptions of two new species of *Keratoisis*. *Mol. Phylogenet. Evol.* 74, 15–28. <https://doi.org/10.1016/j.ympev.2014.01.031>
- Dugal, L., Thomas, L., Wilkinson, S.P., Richards, Z.T., Alexander, J.B., Adam, A.A.S., Kennington, W.J., Jarman, S., Ryan, N.M., Bunce, M., Gilmour, J.P., 2022. Coral monitoring in northwest Australia with environmental DNA metabarcoding using a curated reference database for optimized detection. *Environ. DNA* 4, 63–76. <https://doi.org/10.1002/edn3.199>
- Edgar, R.C., 2004. MUSCLE: Multiple sequence alignment with high accuracy and high throughput. *Nucleic Acids Res.* 32, 1792–1797. <https://doi.org/10.1093/nar/gkh340>

- Erickson, K.L., Pentico, A., Quattrini, A.M., McFadden, C.S., 2021. New approaches to species delimitation and population structure of anthozoans: Two case studies of octocorals using ultraconserved elements and exons. *Mol. Ecol. Resour.* 21, 78–92.
<https://doi.org/10.1111/1755-0998.13241>
- Etnoyer, P., Warrenchuk, J., 2007. A catshark nursery in a deep gorgonian field in the Mississippi Canyon, Gulf of Mexico. *Bull. Mar. Sci.* 81, 553–559.
- Everett, M.V., Park, L.K., 2018. Exploring deep-water coral communities using environmental DNA. *Deep-Sea Res. Part II Top. Stud. Oceanogr.* 150, 229–241.
<https://doi.org/10.1016/j.dsr2.2017.09.008>
- Faircloth, B., 2013. Illumiprocessor: a trimmomatic wrapper for parallel adapter and quality trimming. <http://dx.doi.org/10.6079/J9ILL>
- Faircloth, B.C., 2016. PHYLUCE is a software package for the analysis of conserved genomic loci. *Bioinformatics* 32, 786–788. <https://doi.org/10.1093/bioinformatics/btv646>
- Faircloth, B.C., Sorenson, L., Santini, F., Alfaro, M.E., 2013. A phylogenomic perspective on the radiation of ray-finned fishes based upon targeted sequencing of Ultraconserved Elements (UCEs). *PLOS ONE* 8, e65923. <https://doi.org/10.1371/journal.pone.0065923>
- France, S.C., 2007. Genetic analysis of bamboo corals (Cnidaria: Octocorallia: Isididae): Does lack of colony branching distinguish *Lepidisis* from *Keratoisis*? *Bull. Mar. Sci.* 81, 323–333.
- France, S.C., Hoover, L.L., 2002. DNA sequences of the mitochondrial COI gene have low levels of divergence among deep-sea octocorals (Cnidaria: Anthozoa). *Hydrobiologia* 471, 149–155.
- Glenn, T.C., Nilsen, R.A., Kieran, T.J., Sanders, J.G., Bayona-Vásquez, N.J., Finger, J.W., Pierson, T.W., Bentley, K.E., Hoffberg, S.L., Louha, S., 2019. Adapterama I: universal stubs and primers for 384 unique dual-indexed or 147,456 combinatorially-indexed Illumina libraries (iTru & iNext). *PeerJ* 7, e7755.
- Grant, R., 1976. The marine fauna of New Zealand: Isididae (Octorallia: Gorgonacea) from New Zealand and the Antarctic. *N. Z. Oceanogr. Inst. Mem.*
- Haverkort-Yeh, R.D., McFadden, C.S., Benayahu, Y., Berumen, M., Halász, A., Toonen, R.J., 2013. A taxonomic survey of Saudi Arabian Red Sea octocorals (Cnidaria: Alcyonacea). *Mar. Biodivers.* 43, 279–291. <https://doi.org/10.1007/s12526-013-0157-4>
- Heestand Saucier, E., France, S.C., Watling, L., 2021. Toward a revision of the bamboo corals: Part 3, deconstructing the Family Isididae. *Zootaxa* 5047, 247–272.
- Heestand Saucier, E., Sajjadi, A., France, S.C., 2017. A taxonomic review of the genus *Acanella* (Cnidaria: Octocorallia: Isididae) in the North Atlantic Ocean, with descriptions of two new species. *Zootaxa* 4323, 359–390. <https://doi.org/10.11646/zootaxa.4323.3.2>
- Herrera, S., Shank, T.M., 2016. RAD sequencing enables unprecedented phylogenetic resolution and objective species delimitation in recalcitrant divergent taxa. *Mol. Phylogenet. Evol.* 100, 70–79. <https://doi.org/10.1016/j.ympev.2016.03.010>
- Junier, T., Zdobnov, E.M., 2010. The Newick utilities: high-throughput phylogenetic tree processing in the Unix shell. *Bioinformatics* 26, 1669–1670.
<https://doi.org/10.1093/bioinformatics/btq243>
- Kalyanamoorthy, S., Minh, B.Q., Wong, T.K., Von Haeseler, A., Jermin, L.S., 2017. ModelFinder: fast model selection for accurate phylogenetic estimates. *Nat. Methods* 14, 587–589.
- Katoh, K., Standley, D.M., 2013. MAFFT multiple sequence alignment software version 7: Improvements in performance and usability. *Mol. Biol. Evol.* 30, 772–780.
<https://doi.org/10.1093/molbev/mst010>
- Kenchington, E., Best, M., Cogswell, A., Macisaac, K., Murillo, F., MacDonald, B., Wareham, V., Fuller, S., Jørgensbye, H., Sklyar, V., Thompson, A., 2009. Coral Identification Guide NAFO Area. *NAFO Sci. Coun. Stud.* 42, 1–35. <https://doi.org/10.2960/S.v42.m1>
- Kükenthal, W., 1919. Gorgonaria Wissenschaftliche Ergebnisse der deutschen Tiefsee-Expedition auf dem Dampfer “Valdivia” 1898–1899, 1–946.
- Kumar, S., Stecher, G., Li, M., Knyaz, C., Tamura, K., 2018. MEGA X: Molecular evolutionary genetics analysis across computing platforms. *Mol. Biol. Evol.* 35, 1547–1549.
<https://doi.org/10.1093/molbev/msy096>

- Lapointe, A., Watling, L., 2022. Towards a revision of the bamboo corals (Octocorallia): Part 5, new genera and species of Keratoisididae from the Tasmanian deep sea. *Zootaxa* 5168, 137–157.
- Lapointe, A., Watling, L., 2015. Bamboo corals from the abyssal Pacific: Bathygorgia. *Proc. Biol. Soc. Wash.* 128, 125–136.
- Laroche, O., Kersten, O., Smith, C.R., Goetze, E., 2020. Environmental DNA surveys detect distinct metazoan communities across abyssal plains and seamounts in the western Clarion Clipperton Zone. *Mol. Ecol.* 29, 4588–4604. <https://doi.org/10.1111/mec.15484>
- Mai, U., Mirarab, S., 2018. TreeShrink: fast and accurate detection of outlier long branches in collections of phylogenetic trees. *BMC Genomics* 19, 23–40.
- Maxwell, J., Taboada, S., Taylor, M.L., 2022. *Gorgoniapolynoe caeciliae* revisited: The discovery of new species and molecular connectivity in deep-sea commensal polynoids from the Central Atlantic. *Deep Sea Res. Part Oceanogr. Res. Pap.* 185, 103804. <https://doi.org/10.1016/j.dsr.2022.103804>
- McCullough, J.M., Joseph, L., Moyle, R.G., Andersen, M.J., 2019. Ultraconserved elements put the final nail in the coffin of traditional use of the genus *Meliphaga* (Aves: Meliphagidae). *Zool. Scr.* 48, 411–418. <https://doi.org/10.1111/zsc.12350>
- McFadden, C.S., Benayahu, Y., Pante, E., Thoma, J.N., Nevarez, P.A., France, S.C., 2011. Limitations of mitochondrial gene barcoding in Octocorallia. *Mol. Ecol. Resour.* 11, 19–31. <https://doi.org/10.1111/j.1755-0998.2010.02875.x>
- McFadden, C.S., France, S.C., Sánchez, J.A., Alderslade, P., 2006. A molecular phylogenetic analysis of the Octocorallia (Cnidaria: Anthozoa) based on mitochondrial protein-coding sequences. *Mol. Phylogenet. Evol.* 41, 513–527.
- McFadden, C.S., Haverkort-Yeh, R., Reynolds, A.M., Halász, A., Quattrini, A.M., Forsman, Z.H., Benayahu, Y., Toonen, R.J., 2017. Species boundaries in the absence of morphological, ecological or geographical differentiation in the Red Sea octocoral genus *Ovabunda* (Alcyonacea: Xeniidae). *Mol. Phylogenet. Evol.* 112, 174–184. <https://doi.org/10.1016/j.ympev.2017.04.025>
- McFadden, C.S., Quattrini, A.M., Brugler, M.R., Cowman, P.F., Dueñas, L.F., Kitahara, M.V., Paz-García, D.A., Reimer, J.D., Rodríguez, E., 2021. Phylogenomics, origin, and diversification of anthozoans (Phylum Cnidaria). *Syst. Biol.* 70, 635–647. <https://doi.org/10.1093/sysbio/syaa103>
- McFadden, C.S., Sánchez, J.A., France, S.C., 2010. Molecular phylogenetic insights into the evolution of Octocorallia: A Review. *Integr. Comp. Biol.* 50, 389–410. <https://doi.org/10.1093/icb/icq056>
- McFadden, C.S., van Ofwegen, L.P., Quattrini, A.M., 2022. Revisionary systematics of Octocorallia (Cnidaria: Anthozoa) guided by phylogenomics. *Bull. Soc. Syst. Biol.* 1.
- Miller, S.A., Dykes, D.D., Polesky, H.F., 1988. A simple salting out procedure for extracting DNA from human nucleated cells. *Nucleic Acids Res.* 16, 1215. <https://doi.org/10.1093/nar/16.3.1215>
- Morrissey, D., Untiedt, C.B., Croke, K., Robinson, A., Turley, E., Allcock, A.L., 2022. The biodiversity of Calcaxonian octocorals from the Irish continental slope inferred from multilocus mitochondrial barcoding. *Diversity* 14. <https://doi.org/10.3390/d14070576>
- Muthye, V., Mackereth, C.D., Stewart, J.B., Lavrov, D.V., 2022. Large dataset of octocoral mitochondrial genomes provides new insights into mt-mutS evolution and function. *DNA Repair* 110, 103273. <https://doi.org/10.1016/j.dnarep.2022.103273>
- Neves, B. de M., Wareham Hayes, V., Herder, E., Hedges, K., Grant, C., Archambault, P., 2020. Cold-water soft corals (Cnidaria: Nephtheidae) as habitat for juvenile basket stars (Echinodermata: Gorgonocephalidae). *Front. Mar. Sci.* 7. <https://doi.org/10.3389/fmars.2020.547896>
- Nguyen, L.T., Schmidt, H.A., Von Haeseler, A., Minh, B.Q., 2015. IQ-TREE: A fast and effective stochastic algorithm for estimating maximum-likelihood phylogenies. *Mol. Biol. Evol.* 32, 268–274. <https://doi.org/10.1093/molbev/msu300>
- Orejas, C., Carreiro-Silva, M., Mohn, C., Reimer, J., Samaai, T., Allcock, A.L., Rossi, S., 2022. Marine animal forests of the world: definition and characteristics. *Res. Ideas Outcomes* 8, e96274.

- Pante, E., Abdelkrim, J., Viricel, A., Gey, D., France, S.C., Boisselier, M.C., Samadi, S., 2015. Use of RAD sequencing for delimiting species. *Heredity* 114, 450–459. <https://doi.org/10.1038/hdy.2014.105>
- Parimbelli, A., 2020. Invertebrate associations with deep-sea corals and sponges on the Irish Continental Margin. University of Padova. <https://doi.org/10.13140/RG.2.2.19977.26726>
- Quattrini, A.M., Faircloth, B.C., Dueñas, L.F., Bridge, T.C.L., Brugler, M.R., Calixto-Botía, I.F., DeLeo, D.M., Forêt, S., Herrera, S., Lee, S.M.Y., Miller, D.J., Prada, C., Rádis-Baptista, G., Ramírez-Portilla, C., Sánchez, J.A., Rodríguez, E., McFadden, C.S., 2018. Universal target-enrichment baits for anthozoan (Cnidaria) phylogenomics: New approaches to long-standing problems. *Mol. Ecol. Resour.* 18, 281–295. <https://doi.org/10.1111/1755-0998.12736>
- Quattrini, A.M., Herrera, S., Adams, J.M., Grinyó, J., Allcock, A.L., Shuler, A., Wirshing, H.H., Cordes, E.E., McFadden, C.S., 2022. Phylogeography of *Paramuricea*: The role of depth and water mass in the evolution and distribution of deep-sea corals. *Front. Mar. Sci.* 9.
- Quattrini, A.M., Rodriguez-Burgueno, E., Faircloth, B.C., Cowman, P., Brugler, M.R., Farfan, G., Hellberg, M.E., Kitahara, M.V., Morrison, C., Paz-Garcia, D.A., Reimer, J.D., McFadden, C.S., 2020. Paleoclimate ocean conditions shaped the evolution of corals and their skeletal composition through deep time. *Nat. Ecol. Evol.* <https://doi.org/10.1038/s41559-020-01291-1>
- Quattrini, A.M., Snyder, K., Purow-Ruderman, R., Seiblit, I.G.L., Hoang, J., Floerke, N., Ramos, N.I., Wirshing, H.H., Rodriguez, E., McFadden, C.S., 2022. Extreme mito-nuclear discordance within Anthozoa, with notes on unique properties of their mitochondrial genomes. *bioRxiv* 2022.10.18.512751. <https://doi.org/10.1101/2022.10.18.512751>
- Quattrini, A.M., Wu, T., Soong, K., Jeng, M.S., Benayahu, Y., McFadden, C.S., 2019. A next generation approach to species delimitation reveals the role of hybridization in a cryptic species complex of corals. *BMC Evol. Biol.* 19, 116. <https://doi.org/10.1186/s12862-019-1427-y>
- Rossi, S., Bramanti, L., Gori, A., Orejas, C., 2017. Animal forests of the world: An overview. *Mar. Anim. For. Ecol. Benthic Biodivers. Hotspots* 1–28. https://doi.org/10.1007/978-3-319-21012-4_1
- Rossi, S., Bramanti, L., Horta, P., Allcock, L., Carreiro-Silva, M., Coppari, M., Denis, V., Hadjoannou, L., Isla, E., Jimenez, C., Johnson, M., Mohn, C., Orejas, C., Ramšak, A., Reimer, J., Rinkevich, B., Rizzo, L., Salomidi, M., Samaai, T., Schubert, N., Soares, M., Thurstan, R.H., Vassallo, P., Ziveri, P., Zorrilla-Pujana, J., 2022. Protecting global marine animal forests. *Science* 376, 929. <https://doi.org/10.1126/science.abq7583>
- Roxo, F.F., Ochoa, L.E., Sabaj, M.H., Lujan, N.K., Covain, R., Silva, G.S.C., Melo, B.F., Albert, J.S., Chang, J., Foresti, F., Alfaro, M.E., Oliveira, C., 2019. Phylogenomic reappraisal of the Neotropical catfish family Loricariidae (Teleostei: Siluriformes) using ultraconserved elements. *Mol. Phylogenet. Evol.* 135, 148–165. <https://doi.org/10.1016/j.ympev.2019.02.017>
- Sanchez, J.A., McFadden, C., France, S., Lasker, H., 2003. Molecular Phylogenetic analyses of shallow-water Caribbean octocorals. *Mar. Biol.* 142, 975–987. <https://doi.org/10.1007/s00227-003-1018-7>
- Shea, E.K., Ziegler, A., Faber, C., Shank, T.M., 2018. Dumbo octopod hatchling provides insight into early cirrate life cycle. *Curr. Biol.* 28, R144–R145. <https://doi.org/10.1016/j.cub.2018.01.032>
- Templeton, A.R., Crandall, K.A., Sing, C.F., 1992. A cladistic analysis of phenotypic associations with haplotypes inferred from restriction endonuclease mapping and DNA sequence data. III. Cladogram estimation. *Genetics* 132, 619–633.
- van der Ham, J.L., Brugler, M.R., France, S.C., 2009. Exploring the utility of an indel-rich, mitochondrial intergenic region as a molecular barcode for bamboo corals (Octocorallia: Isididae). *Mar. Genomics* 2, 183–192. <https://doi.org/10.1016/j.margen.2009.10.002>
- Vecchione, M., 2019. ROV Observations on Reproduction by Deep-Sea Cephalopods in the Central Pacific Ocean, *Frontiers in Marine Science*.
- Watling, L., 2015. A new genus of bamboo coral (Octocorallia: Isididae) from the Bahamas. *Zootaxa* 3918, 239–249.
- Watling, L., France, S.C., 2021. Toward a revision of the bamboo corals: Part 2, untangling the genus *Lepidisis* (Octocorallia: Isididae). *Bull. Peabody Mus. Nat. Hist.* 62, 97–110.

- Watling, L., France, S.C., 2011. A new genus and species of bamboo coral (Octocorallia: Isididae: Keratoisidinae) from the New England seamounts. *Bull. Peabody Mus. Nat. Hist.* 52, 209–221.
- Watling, L., France, S.C., Pante, E., Simpson, A., 2011. Biology of deep-water octocorals, in: Lesser, M.B.T.-A. in M.B. (Ed.), *Advances in Marine Biology*. Academic Press, pp. 41–122. <https://doi.org/10.1016/B978-0-12-385529-9.00002-0>
- Watling, L., Heestand Saucier, E., France, S.C., 2022. Towards a revision of the bamboo corals (Octocorallia): Part 4, delineating the family Keratoisididae. *Zootaxa* 5093, 337–375.
- Zhang, C., Rabiee, M., Sayyari, E., Mirarab, S., 2018. ASTRAL-III: Polynomial time species tree reconstruction from partially resolved gene trees. *BMC Bioinformatics* 19, 153. <https://doi.org/10.1186/s12859-018-2129-y>

TABLES

Table 1. Alignment summary data for each dataset used in phylogenomic analyses.

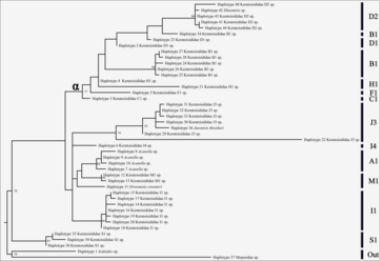
Dataset	Method	Taxa	#Loci	Mean Locus Length (bp)	Total Alignment Length (bp)
<i>mtMutS</i>	IQTree	152 individuals – represented by 44 haplotypes	1	742	879
50% matrix	IQTree and ASTRAL III	121	1729	1326	2292009
75% matrix	IQTree and ASTRAL III	121	231	1625	375337

FIGURE LEGENDS

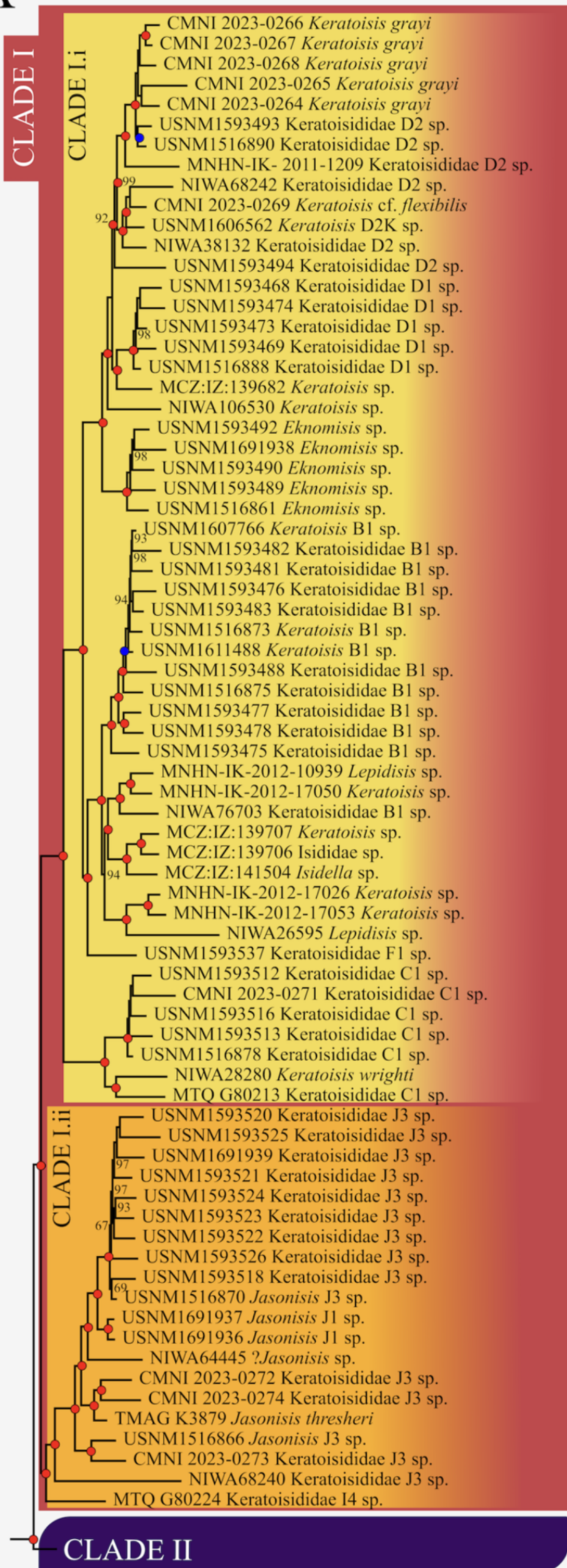
Figure 1. A maximum likelihood tree of all 44 recovered haplotypes, representing 152 individuals, based on an 879 bp *mtMutS* alignment. Bootstrap values less than 75 are not reported.

Figure 2. Maximum likelihood trees constructed from A) the 50% conserved elements taxon occupancy matrix (1729 loci) and B) the 50% occupancy matrix (231 loci). All nodes represent 100% ultrafast bootstrap support unless otherwise stated. The colour of each node represents the transposed ASTRAL local posterior probability values. Red indicates maximum LPP support (1), blue is $\geq 0.9 < 1$ LPP, and white is $\geq 0.75 < 0.9$ LPP. Nodes with no coloured circle indicate a relationship that was not recovered by ASTRAL. The dashed line represents a branch that was manually shortened for visualisation purposes. A1, B1, C1, D1, D2, F1, H1, I1, I4, J3, M1, and S1, refer to the keratoisidid groups defined by Watling et al. 2022).

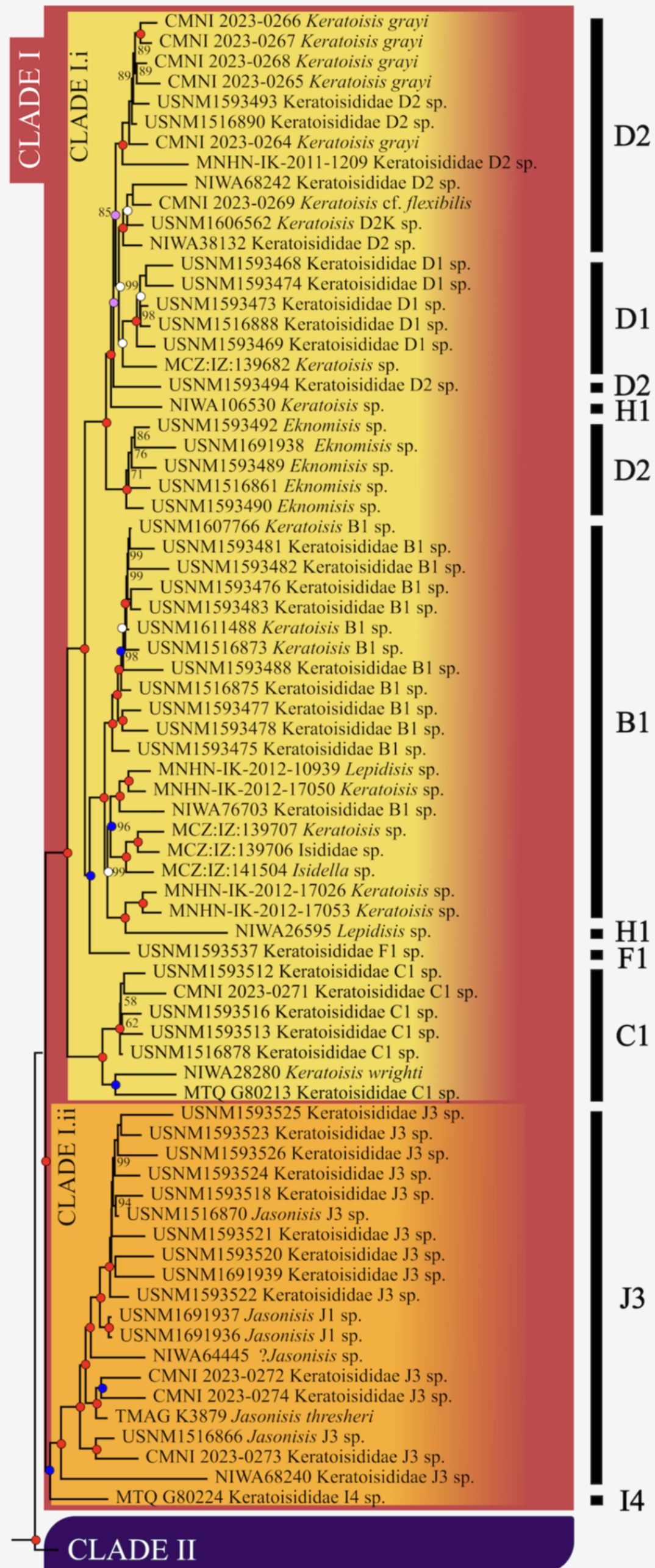
Figure 3. Morphological characters characteristic of each subclade, adapted from Watling et al. (2022). The Cladogram represents the relationships among groups as recovered by the 50% taxon occupancy matrix ML phylogenetic analyses. Members assigned to subclades D2, H1, and M1 were not recovered as monophyletic and so appear more than once in the cladogram.



A

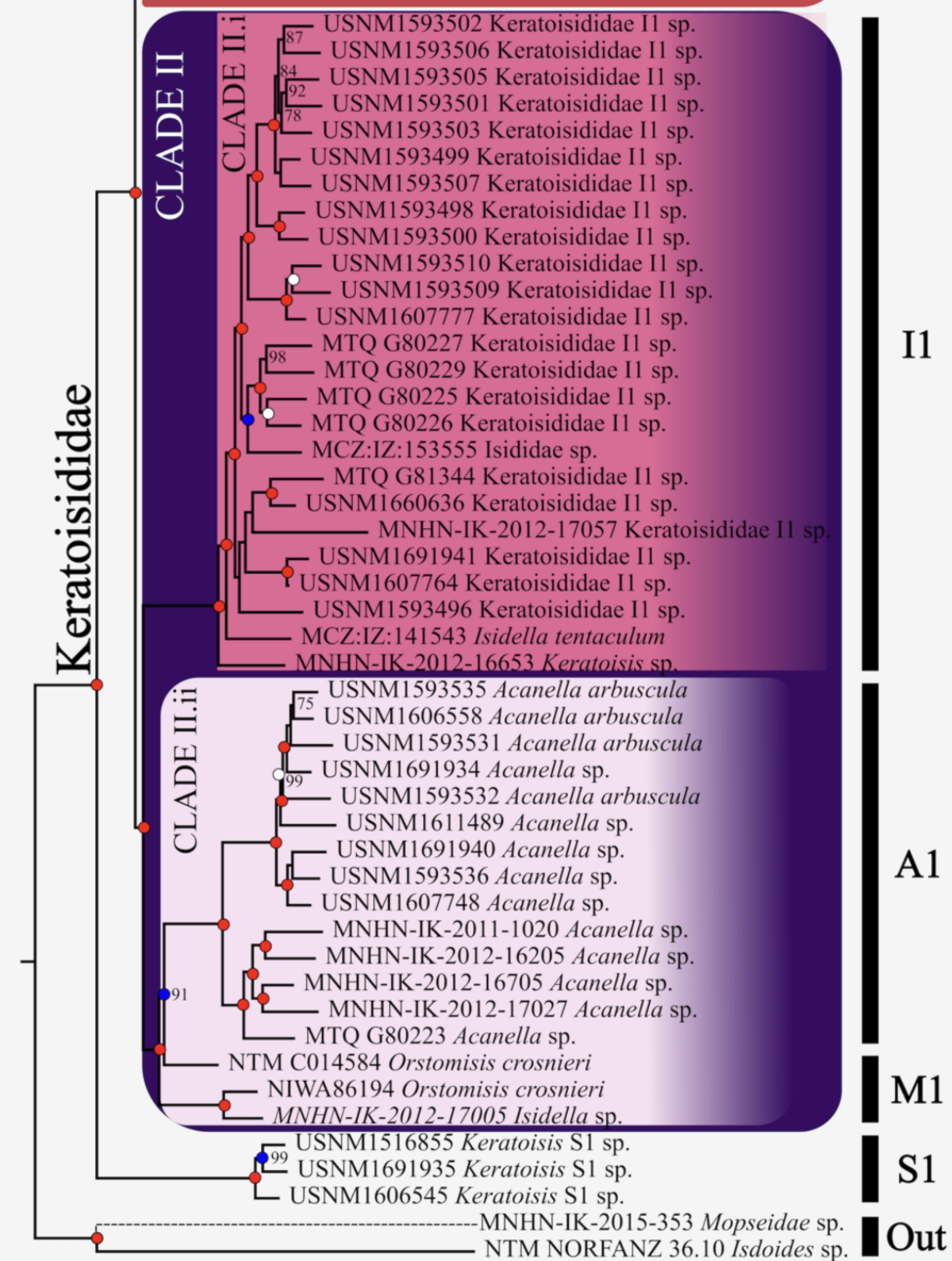


B



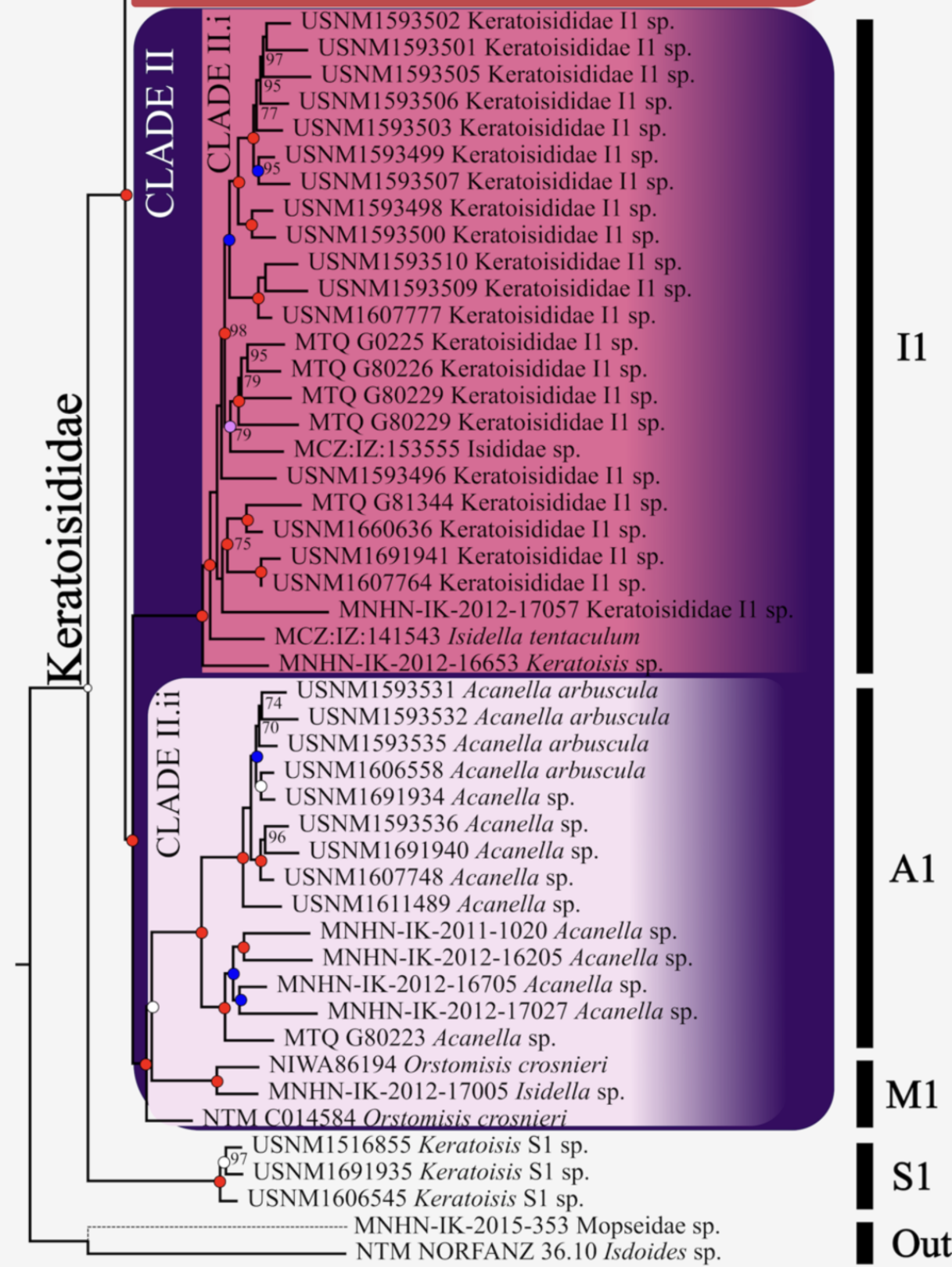
A

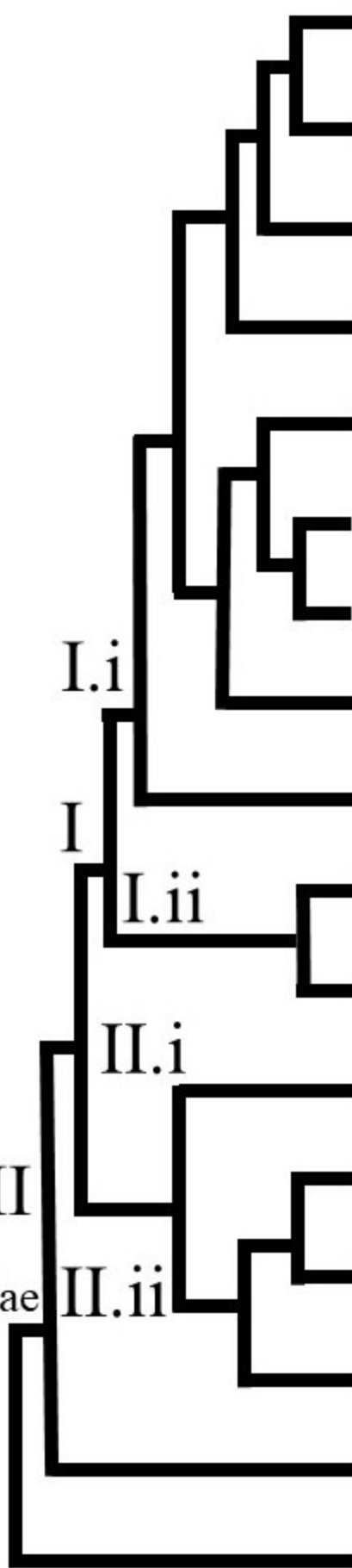
CLADE I



B

CLADE I



		Group/ Lineage ID	Branching Pattern	Colony Morphology	Polyp Sclerites composition	Coenenchyme thickness
 <p>Keratoisididae</p>		D2	None/Internodal	Whip/Flabellate/ Open Bush	Needles and rods, both upper and lower polyp	Thick/Thin
		D1	None/Internodal	Whip/Densely branched planar	Needles, few in lower polyp	Thick/Thin
		H1	Internodal	Planar flabellate	Needles	Moderately Thick
		D2	None/Internodal	Whip/Flabellate/ Open Bush	Needles and rods, both upper and lower polyp	Thick/Thin
		B1	None/Internodal	Whip/Planar flabellate	Rods/Needles/som etimes scales	Thick
		B1	None/Internodal	Whip/Planar flabellate	Rods/Needles/som etimes scales	Thick
		H1	Internodal	Planar flabellate	Needles and scales	Moderately Thick
		F1	None/Internodal/ nodal	Whip/sparsely- branching from base	Needles and rods	Thin
		C1	none	Whips – distal coiling possible	Needles	Thick
		J3	Nodal and/or Internodal	Whips/Planar/ Bramble bush	Needles, rods, flat rods, and scales	Thick/Thin
		I4	Nodal	Whip to trident to candelabra	Needles, no sclerites in bottom half of polyp	Thick
		I1	Nodal	Whip/Planar fan	Needles, scales are rare	Thin
		A1	Nodal	Bush/Flabellate	Needles and rods	Thin
		M1	Nodal	Multiplanar flabellate	rods	Thin
		M1	Nodal	Multiplanar flabellate	rods	Thin
		S1	Nodal/Internodal	Whip/Open structure of long branches	Rods and curved rods	Thin
		OUT				